

Test-rig for the determination of coefficients of sliding friction under the influence of abrasive intermediate materials

by Christian Segieth and Wolfgang Poppy

The tracked drives of earthmoving vehicles are subject to high levels of wear due to the abrasive nature of the working material. This results in very high costs for spare parts which, over the machine's complete service life, can equal its replacement cost. Before attempts can be made to reduce the wear in the tracked drive, it is important to experimentally determine the tribological parameters affecting the system. This article describes the development of a test-rig in which these parameters can be investigated under realistic simulated conditions, taking into account the effect of various abrasive materials. The method includes an interesting application of force and measurement transducers.

The measurement problem

The drives of bulldozers and loading shovels are subject to high levels of alternating loads which lead to substantial wear on the drive components. The main points of wear are the teeth on the sprocket and the chain bushings. Particularly high levels of wear occur when operating in abrasive ground containing quartz and where the ground is covered with water. **Figure 1** shows a bulldozer in use spreading a silica sand/water mixture. Wear in the drives of earthmoving equipment causes high replacement costs which, through the complete service life, can amount up to 100% of the cost of a new unit.

In order to be able to systematically reduce the wear, it is necessary to determine the tribological conditions affecting the combination of chain bushing and sprocket teeth, including all the parameters which influence the wear. On lubricated chain drives frictional forces are normally neglected when applying the well known methods of calculating the tooth-meshing forces [3,4]. This simplification is not possible for the tracks of earthmoving vehicles because the abrasive pieces of earth entering the chain drive produce significant increases in the friction. A new computational model was developed to take into account the frictional forces during the computation of the tooth-meshing forces between the bushing and the tooth and also between the bushing and the pin. Knowledge about the coefficients of sliding friction for both frictional points is required for the computations.

The coefficients of sliding friction are known for unlubricated and lubricated steel-to-steel frictional systems. The coefficients required for the computation of the tooth meshing forces on the drives of earthmoving

equipment on the basis of steel-to-steel with an intermediate abrasive material could previously only be estimated. A railway engineering publication provided some information about the increased frictional effects of sand used during braking [6].

The need to verify the assumptions made for the coefficients of sliding friction during the computation of the meshing forces led in turn to the extension of a wear test-rig, enabling the measurement of the coefficients under conditions similar to those in use. The test-rig was



Fig. 1: Bulldozer in operation on ground covered by water.

originally developed for investigations into wear on earthmoving vehicles. Attempts were made to measure the coefficients of sliding friction in dependence of the most important parameters. These tests were conducted on specimens formed from materials used on the drives of factory-produced earthmoving vehicles.

Simulation test-rig

A servo-hydraulically driven simulation test-rig was developed in order to be able to investigate the effect of a number of variables on the wear of the bushings and teeth in isolation of one another and under reproducible conditions. It was designed for tests on the popular D6 size of drive found on bulldozers with 16.5 t (16.2 tons) operational weight and 115 kW drive power. The most important demands made of this test-rig were as follows:

- the force and movement of the bushing/tooth contact should be simulated as in use according to time variations as found by analytical computations [5],
- silica sand which was to be used as the intermediate material should be dosed and fed to the system in a reproducible manner,
- normal forces and frictional forces should be separated from one another as far as possible to avoid mutual effects.

Since the chain bushing, as can be seen in **Fig. 2** in the unworn state, is applied to the straight face of the tooth, it was replaced in the test-rig by a simply produced plane test element (flat specimen of width 80 mm/3.2 in). Instead of the chain bushing, a cylindrical element with the same external diameter was used in the test-rig (round specimen of 69 mm/2.7 in diameter). **Figure 3** shows a photograph of the flat and round specimens on the test-rig. Traces of wear can be clearly seen.

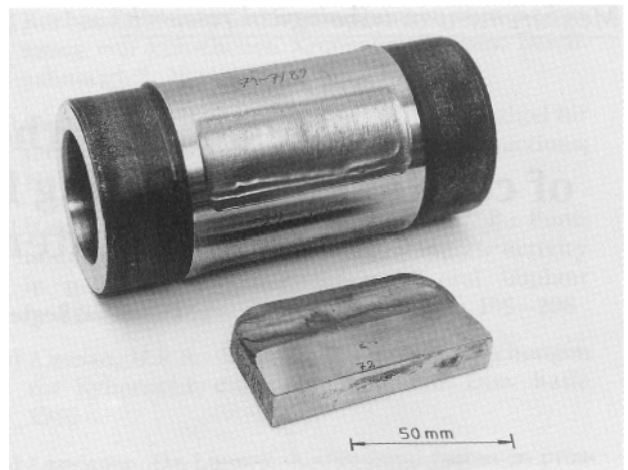


Fig. 3: Round and flat specimens showing traces of wear produced in the test-rig

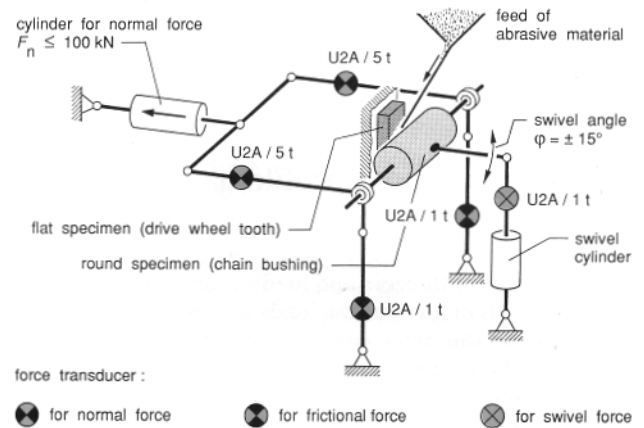


Fig. 4: Operating principle of the test-rig for the determination of the coefficients of sliding friction

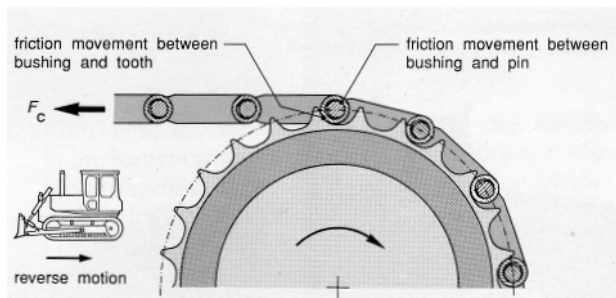


Fig. 2: Engaging action of the track chain in the drive sprocket when driving in reverse

The basic principle of the test-rig is shown in **Fig. 4**. A hydraulic cylinder producing the normal force F_n pulls the cylindrical element, i.e. the round specimen which simulates the chain bushing, against the flat specimen representing the sprocket tooth. The round specimen is rotated backwards and forwards by the swivel cylinder through the swivel angle, rubbing against the flat specimen. The axle of the round specimen is joined to guides

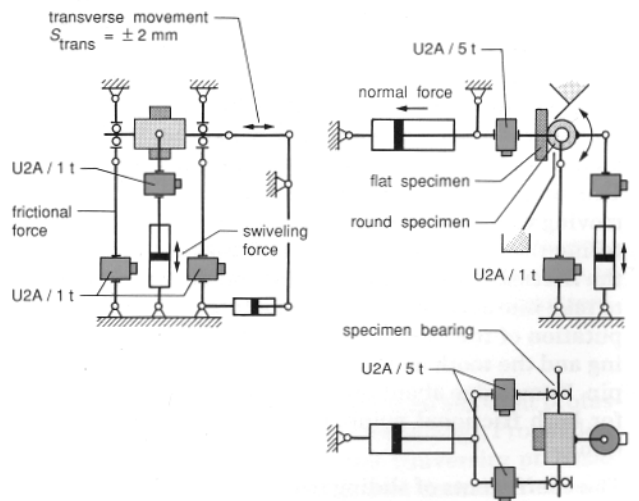


Fig. 5: Test-rig design and arrangement of the force transducers

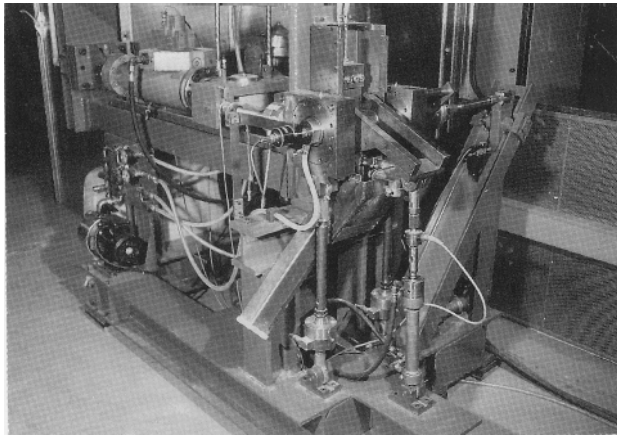


Fig. 6: Photograph of the test-rig

so that the round specimen does not roll on the flat one, but rubs against it instead. The swivel angle corresponds to the pitch angle of the drive sprocket. Abrasive intermediate material is fed into the contact zone and flows downwards. The round specimen can be pushed against the flat specimen in the transverse direction with another hydraulic cylinder. This ensures that the same points are not always in contact with one another.

The normal, frictional and swiveling forces are measured on the test-rig. The arrangement of the force transducers built into the rig can be seen in Fig. 5. The normal force, which is transferred by a two-part force introduction yoke, is measured by two force transducers of the type U2A, each with 50 kN (11,240 lbf) nominal load. The swiveling forces are transferred via a U2A force transducer with 10 kN (2248 lbf) nominal load. The two U2A/ 50 kN Force Transducers for measuring the frictional force are built into the round specimen and secured against rolling by two guides. Figure 6 shows a photograph of the test-rig.

The complete test-rig is driven servo-hydraulically and is controlled by an IBM compatible computer. As shown schematically in Fig. 7, the cylinder for the normal force is provided with a servo-valve and a combined force and displacement control system including an adjustable limit. The swivel cylinder and the cylinder for the transverse movement are controlled via servo-valves and P controllers. And so, for the first time in tribological research, a test-rig has been able to produce almost any, even stochastic variations of normal force and sliding movements with time. Also, maximum forces of up to 100 kN (22,480 lbf) are possible.

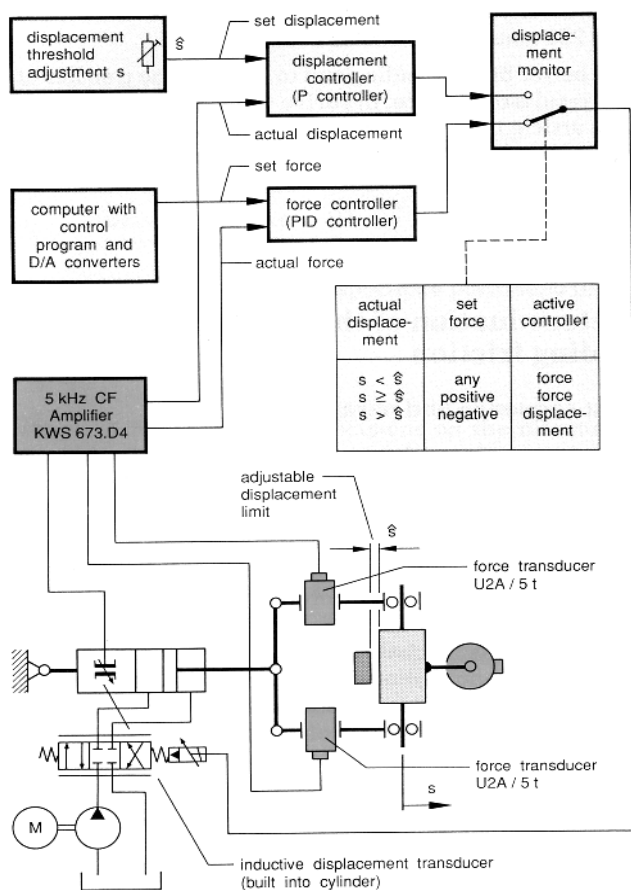


Fig. 7: Combined force/displacement control for the cylinder producing the normal force incorporating automatic displacement limit monitoring

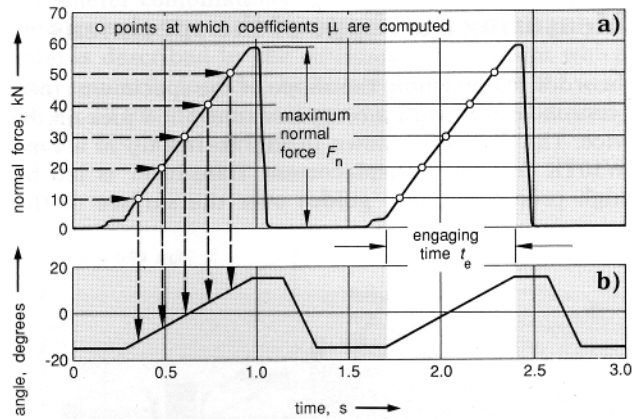


Fig. 8: Test cycle with increasing force for simulating the engaging of the bushing in the sprocket and for the measurement of the coefficients of sliding friction μ between the round and flat specimens (chain bushing and drive-sprocket tooth)

- a) variation of force with time
- b) variation of the swivel angle with time

Force regulation is usually active for the normal force cylinder. With negative set values, this leads to the round specimen lifting from the flat specimen. The cylinder displacement is continuously monitored to ensure that it does not collide with the protective cubicle enclosing the testing area. If the set threshold displacement is exceeded, a changeover occurs from force control to displacement control. The round specimen remains at the set distance. For positive set force values, the round specimen is again moved to the flat specimen. Using this force control combined with displacement limiting, it is possible to control the variation of the normal force with time and the lifting of the round specimen from the flat specimen at the end of each test cycle.

A test cycle corresponding to the engaging of the chain bushing in the sprocket when driving backwards is characterized by the maximum normal force F_n between the round and flat specimens at the end of the swivel movement and the engaging time t_e . **Figure 8** shows in the upper part the time variations of the normal force and in the lower part the swivel angle measured with a potentiometric angular sensor.

The engaging time can be calculated from the driving velocity v of the bulldozer and the chain pitch p . During the rotation of the round specimen, i.e. chain bushing, with constant angular velocity, the normal force is increased linearly and then reduced at the end of the rotation. Then the round specimen is raised 3 mm (0.12 in) from the flat specimen, i.e. the tooth, so that fresh abrasive material can enter the contact zone. Simultaneously, the round specimen is rotated back and again pulled onto the flat specimen. The next test cycle begins. This test cycle was also used for the measurement of the coefficients of sliding friction; the points for which the coefficients have been calculated have been entered in **Fig. 8**.

Measuring the shape of the specimens

In order to determine the shape of the specimens, they were measured with a computer-controlled pick-up device. The device is shown in **Fig. 9**. The tip of a type W10TK Inductive Displacement Transducer is led by high precision linear guides over the surface of the

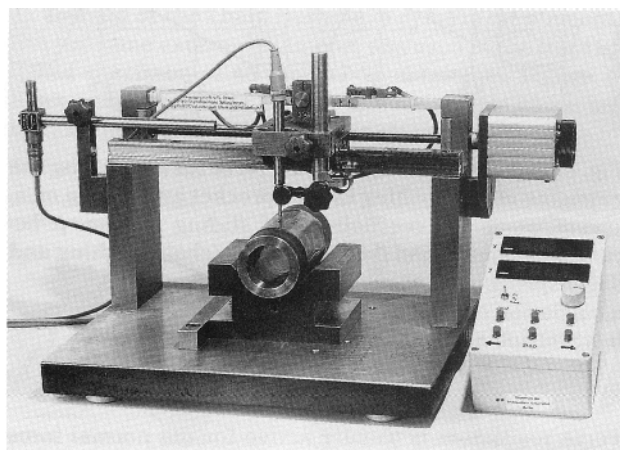


Fig. 9: Probe device for the two-dimensional measurement of the wear W_q on the round and flat specimens

specimen. Another inductive displacement transducer, type W50, measures the travel of the displacement pickup. The maximum values of travel for the displacement transducers produce a measurement range of 10 mm (0.4 in) in height and 100 mm (4 in) in length. The accuracy of the measurement equipment is better than $5 \mu\text{m}$ (0.2 mils) over a 25 mm (1 in) horizontal sampling displacement.

From the measurement data obtained in the abrasion tests, the abraded mass $W_{m/sw}$ is calculated for one swivel movement, i.e. test cycle. For the measurement of the coefficients of sliding friction, a check is made with the pick-up device of whether the shape of the specimen still corresponds to that on which the computational formulas are based.

Tribological load on the chain bushing and drive sprocket

The tribological load on the friction system formed by the chain bushing and the drive sprocket is represented by the transferred normal force F_n , the resulting Hertzian surface pressure σ and the sliding velocity v_s which is dependent on the driving velocity. For bulldozers with the size of drive on which the investigations were based, the threshold values for the loads in the complete range of applications were 15 kN (3372 lbf) and 60 kN (13,488 lbf) for the normal force at driving velocities of 2 km/h and 8 km/h respectively (1.24 and 5 mph). The corresponding values for the Hertzian surface pressure were 300 N/mm^2 and 850 N/mm^2 (43,509 and 123,277 lbf/in²).

The sliding velocity v_s can be calculated from the driving velocity and varies in the range between 50 mm/s and 250 mm/s (2 in/s and 10 in/s).

For better understanding and to simplify the transfer of the results to practice, the drive velocities are quoted in this article instead of the sliding velocities. The conversion to sliding velocity simplifies comparison with other tribological investigations.

Determination of the coefficients of sliding friction

Test sequence and parameters

Care was taken during the determination of the coefficients of sliding friction to ensure that the variation of force and movement corresponded as closely as possible to the engaging of the chain bushing in the sprocket when driving in reverse. Therefore, the test cycle shown in **Fig. 8** was used with increasing force. All forces and movements on the chain bushing were measured during the test procedure. Since the forces on the left-hand and right-hand bearings of the round specimen were the same, the plane model shown in **Fig. 10** was formed. The coefficient of sliding friction μ , the bearing-friction coefficient μ_b and the normal force F_n in the contact zone were calculated using the equations given in [1] from the equilibrium of forces on the round specimen.

Since the angular velocity of the round specimen is constant during swiveling, forces due to acceleration could be neglected in the computation. Also, the misalignment of the swivel cylinder could be neglected since the angle was always smaller than 0.4° .

The coefficient of sliding friction μ was calculated when the normal force during the test cycle exceeded the values 10 kN, 20 kN, 30 kN, 40 kN and 50 kN (2248 lbf 11,240 lbf). Ten test cycles were evaluated and the mean coefficient was calculated for each simulated driving velocity, then the coefficient values for the next driving velocity were determined. In order to eliminate the varying effects of the engaging process, the tests were repeated and evaluated with the three driving velocities for each pair of specimens.

The equations for the calculation of the coefficients of sliding friction are not valid if the specimen shape alters as a result of the abrasion. The effect of the modified

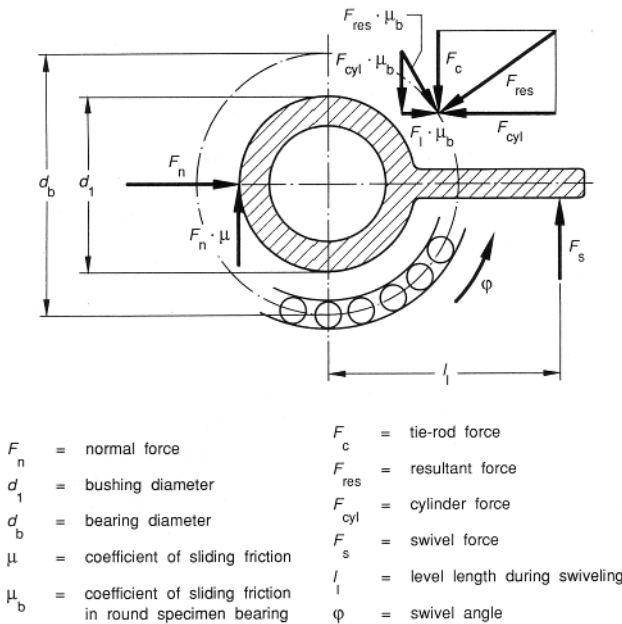


Fig. 10: Forces on the round specimen positioned in the test-rig

shape of round and flat specimens on the measuring error during the determination of the coefficients has already been thoroughly investigated [7]. The shape of the test specimens was continuously monitored and the experiments were interrupted when it appeared that measurement errors > 5 % would be produced. The test specimens were cleaned and degreased each time before the shape was measured.

In order to measure the coefficients of sliding friction under conditions similar to the actual operating conditions, parameters were selected which covered the field of application of the bulldozers investigated. A total of two pairings of specimen material were investigated with four different intermediate material combinations. The first combination consisted of the material SAE 15B15Cr for the round specimen and 35Mn5Cr for the flat specimen. Both materials are often used in production. For comparison, a pairing of specimens in the familiar 42CrMo4 was also included.

Two test specimen pairings were investigated for each pairing of specimen material and for each abrasive ma-

terial. Using specimens made from the above mentioned materials often used in bulldozers, the following combinations were tested:

- without any intermediate material
- with silica sand as abrasive intermediate material
- with water as intermediate material
- with water and silica sand as intermediate material.

The first two combinations of intermediate material were tested using test specimens in the material 42CrMo4 for comparison purposes. A total of 14 individual tests were carried out.

A method was required to enable the effect of the normal force F_n and the driving velocity v on the coefficients of sliding friction μ be better assessed. A regression polynomial of the second order with bilinear components was used as an approximation taking the measuring points of both tests for one combination of intermediate materials [8].

$$\mu = a_0 + a_1 \cdot F_n + a_2 \cdot v + a_3 \cdot F_n \cdot v + a_4 \cdot F_n^2 + a_5 \cdot v^2$$

The polynomial was then displayed graphically as a curved surface. The result of the regression computation can be interpreted as the mean of the separate parameter combinations, taking all the measurements into account. The accuracy of the approximation polynomial is described by the correlation coefficient which was generally found to be better than $r \geq 0.9$. If r were unity, all the measurements would be situated directly on the displayed surface.

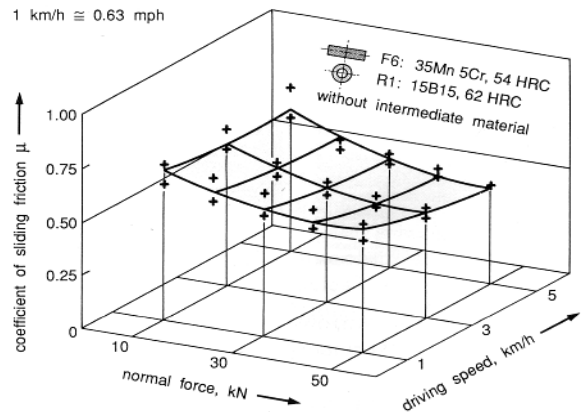


Fig. 11: Example of a display of the results; coefficients of sliding friction for one combination of component materials without intermediate material in dependence of normal force and driving velocity

Coefficients of sliding friction without abrasive intermediate material

The coefficients for the material combinations normally used in production (SAE 15B15Cr and 35Mn5Cr) are shown in Fig.11 which is an example of the display of the results. In the investigated range of parameters under

dry friction conditions without any intermediate material, values between 0.44 and 0.75 were produced for the coefficients. Here the normal force had a substantial effect on the coefficient. The coefficient reduced with increasing normal force. The driving velocity and hence the sliding velocity had only a slight effect which could be neglected.

The worn abraded shapes of the round and flat specimens after the tests were very similar to one another. It is therefore sufficient to observe the surface of the specimens. **Figure 12** shows examples of four worn shapes. After tests without intermediate material, the appearance after wear was relatively smooth (**Fig. 12a**) and a few deposits of brown frictionally oxidized iron were apparent. After the test without intermediate material, the surface of the specimen exhibited a relatively low degree of roughness with $R_t = 18 \mu\text{m}$ (0.7 mils) in comparison to the tests with silica sand as the abrasive intermediate material. Due to the process of material being transferred, welded and then torn away, some furrows were formed in the surface. Adhesion was the main process responsible for wear. The wear on the test specimens was so small that it could not be measured with the measurement equipment.

With the second combination of materials, i.e. both specimens in 42CrMo4, the coefficients of sliding friction for dry friction without abrasive intermediate material was

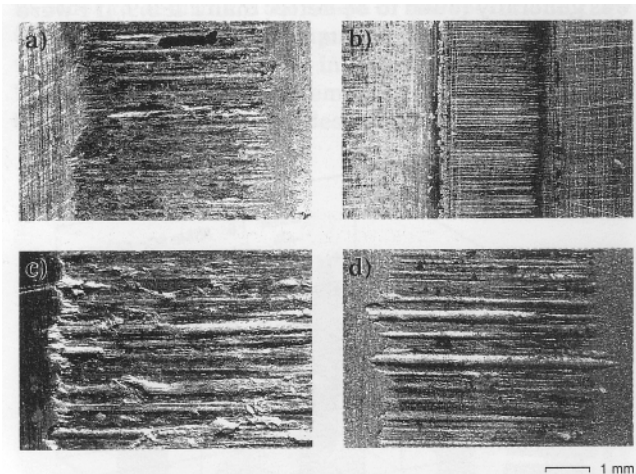


Fig. 12: Surfaces of various flat specimens (35Mn5Cr, 54 HRC) after measurement of the coefficients in the test-rig

- a) without intermediate material
- b) only water as intermediate material
- c) only silica sand as intermediate material
- d) silica sand and water as intermediate materials

between 0.41 and 0.58. The same falling trend was observed for increasing normal force and the driving speed was again found to have no effect. This combination of component material led to scoring and extreme wear at high surface pressures at the end of the test cycle. This meant that only one test could be carried out and it was not possible to find a regression polynomial. When water was added, the coefficients were lower than for dry friction and were between 0.36 and 0.45 for the

first combination of component materials. In contrast to the case for dry friction, there was a more gradual rise in the coefficients with increasing normal force. The surfaces showed no traces of transfer of component material or frictional oxidation (**Fig. 12b**). Furrows due to the rotation of the harder round specimen were formed on the softer flat specimen. Roughness in the surface was smoothed out due to the friction process so that the surface roughness on both the round and flat specimens was less after the test than before the test. The lower coefficients of sliding friction compared to the dry case can be explained by the water lubricating the surfaces and reducing the effect of adhesion as a friction process, a process which had such a pronounced effect in the case of dry friction.

Coefficients of sliding friction with abrasive intermediate material

When silica sand was introduced into the friction zone, the coefficients of sliding friction for the first combination of component materials were smaller than for dry friction. The values for μ were situated between 0.39 and 0.55. With increasing normal force the coefficients were reduced in an almost linear manner. The sliding velocity had no effect in the range under investigation. Reduced coefficients with increasing surface pressure were also found during other investigations with silica sand as the intermediate material [9].

Silica sand in the friction zone separates the surfaces of the friction components so that the friction and wear process is more one of micro-plowing and micro-machining, i.e. abrasion, than one of adhesion. The surface of the flat specimen exhibited deep furrows with plastic deformation of the component material resulting from the micro-plowing and machining (**Fig. 12c**). A few scaly areas where transfer of material occurred due to adhesion could also be observed. A burr was formed due to plastic deformation at the end of the friction zone as a consequence of the high surface pressure.

The coefficients of sliding friction for the second combination of component materials were not very different from those found for the first combination. With silica sand as the intermediate material, the tendency to scoring as found with dry friction was no longer present.

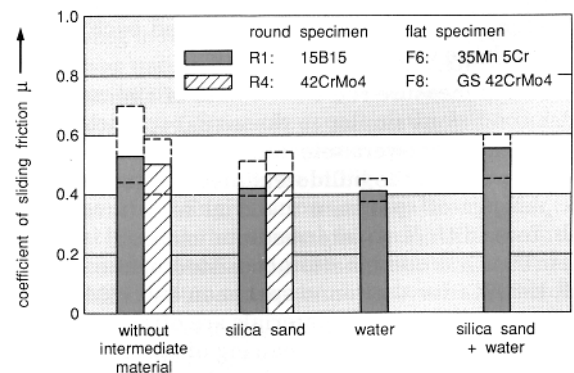


Fig. 13: Mean coefficients of sliding friction as found with the test-rig

When water was introduced into the friction zone in addition to silica sand, the coefficients for the first combination of component materials were greater than with no water. The coefficients were between 0.45 and 0.62. The reasons for the increase in the frictional effect of the water could not be found. The surfaces exhibited a similar appearance as for dry sand, i.e. pronounced furrows due to micro-plowing and machining (**Fig. 12d**). The maximum surface roughness was similar to the test with just silica sand and no water. Regions with adhesion and welding of the surfaces were not found.

Coefficients of sliding friction in designing bulldozer drives

When computing the meshing forces for bulldozer drives, it is not important to state the individual coefficients of sliding friction in dependence of the parameters mentioned above, because these can only be estimated for practical applications. It is more important therefore, to state a range in which the coefficients are most likely situated, based on the measurements described in the last three sections.

The mean coefficients for all investigated parameter combinations determined with the regression calculation are shown in **Fig. 13**. They are in the range $0.4 \leq \mu \leq 0.7$. The values for $\mu > 0.6$ were only obtained for the bulldozer drives with dry friction, but with degreased and ground surfaces. These conditions are not really relevant from an application point of view. Therefore, figures of $0.4 \leq \mu \leq 0.6$ can be assumed for the coefficients of sliding friction at the contact point of the bushing/ drive-sprocket tooth when designing bulldozer drives.

Conclusion

When calculating the meshing forces on the tracked drives of earthmoving vehicles, the frictional force between the chain bushing and the tooth must be considered. The magnitude of this force is affected significantly by abrasive materials in the drive meshing system. Since the relevant coefficients of sliding friction are unknown, a servo-hydraulic test-rig was set up for investigating the wear on bulldozer drives.

The measurements were carried out with full-scale test specimens in the original component materials. The parameters which substantially affected the coefficients of sliding friction were varied. These parameters were the normal force, sliding velocity and the water content of the abrasive silica sand. It was found that values between 0.4 and 0.6 for μ , the coefficient of sliding friction at the contact point of the chain bushing/ drive sprocket tooth, can be assumed in the design of tracked vehicle drives.

References

- [1] Segieth, C.: Verschleißuntersuchungen an Raupenlaufwerken von Baumaschinen; Dissertation, Tech. Univ. Berlin, 1990
- [2] Poppy, W., Faß, G., Segieth, C.: Verschleißminderung und Lebensdauerverlängerung bei Raupenlaufwerken von Baumaschinen; Research Report (Part 1) on Design of Construction Equipment, Tech. Univ. Berlin, 1988
- [3] Rachner, H-G.: Stahlgelenk Ketten und Kettengetriebe; Springer-Verlag, Berlin, Heidelberg, New York, 1962
- [4] Worobjew, N.: Grundlagen der Kettentriebe; VEB-Verlag Technik, Berlin, 1971
- [5] Segieth, C., Poppy, W.: Verzahnungskräfte an Raupenlaufwerken von Baumaschinen; Konstruktion 42 (1990) 4, pp. 127 – 134
- [6] Bugarcic, H.: Optimierung von Sandstreueinrichtungen bei Stadtbahnfahrzeugen; Final report of research project commissioned by the Federal Minister of Transport, Minister of Transport for North Rhine-Westphalia and the Essener Verkehrs AG, Tech. Univ. Berlin, 1980
- [7] Wirries, D.: Tribologische Modelluntersuchungen zur Ermittlung der Lebensdauer von Streckkettenpaarungen; Dissertation, Tech. Univ. Berlin, 1988
- [8] Wolfe, P.M., Koelling, C.P.: BASIC-Programm aus Naturwissenschaft und Technik; Carl Hanser Verlag Munich, Vienna, 1985
- [9] Günther, H.: Untersuchungen zum Verschleißverhalten metallischer Gleitpaarungen unter Berücksichtigung der abrasiver Zwischenstoffe; Dissertation, Bergakademie Freiberg, 1981

Acknowledgement

This article is a summary of the dissertation in [1]. The tests were conducted with the support of Intertractor Viehmann GmbH & Co. of Gevelsberg, FRG within the scope of the research project "Abrasive wear on machines used in the construction industry — Section: Reducing wear and increasing the service life of track drives on construction vehicles". The project was promoted by the Federal Minister for Research and Technology (BMFT) [2].

Dr.-Ing. Christian Segieth was formerly on the staff of the Technical University, Berlin, FRG working in the specialist section Design of Construction Machines which is headed by **Prof. Dr.-Ing. Wolfgang Poppy**. Dr. Segieth is now with AEG Westinghouse Transport-Systeme GmbH, Berlin.